A HYBRID BOUNDARY–REGION LEFT VENTRICLE SEGMENTATION IN COMPUTED TOMOGRAPHY

Antonio Bravo, José Clemente
Grupo de Bioingeniería, Decanato de Investigación, Universidad Nacional Experimental del Táchira
San Cristóbal 5001, Venezuela

Miguel Vera, José Avila, Rubén Medina
Grupo de Ingeniería Biomédica, Facultad de Ingeniería, Universidad de Los Andes, Mérida 5101, Venezuela

Keywords: Segmentation, Generalized Hough transform, Mathematical morphology, Unsupervised clustering, Cardiac images, Left ventricle.

Abstract: An automatic approach based on the generalized Hough transform (GHT) and unsupervised clustering technique to obtain the endocardial surface is proposed. The approach is applied to multi slice computerized tomography (MSCT) images of the heart. The first step is the initialization, where a GHT–based segmentation algorithm is used to detect the edocardial contour in one MSCT slice. The centroid of this contour is used as a seed point for initializing a clustering algorithm. A two stage segmentation algorithm is used for segmenting the three–dimensional MSCT database. First, the complete database is filtered using mathematical morphology operators in order to improve the left ventricle cavity information in these images. The second stage is based on a region growing method. A seed point located inside the cardiac cavity is used as input for the clustering algorithm. This seed point is propagated along the image sequence to obtain the left ventricle surfaces for all instants of the cardiac cycle. The method is validated by comparing the estimated surfaces with respect to left ventricle shapes drawn by a cardiologist. The average error obtained was 1.52 mm.

1 INTRODUCTION

In medical image processing, segmentation is an important tool to analyze anatomic tissue features types, and spatial distribution of functional regions (active and pathological) (Bankman, 2000). Additionally, this technique is useful to extract information for diagnosis or quantification (Angelini et al., 2001), visualization (Nelson and Elvins, 1993), and finally compression, storage and transmission (Field, 1996; DICOM, 1999).

Image segmentation techniques are based on the organization and grouping of a set of shapes, being the proximity, similarity and continuity the main organization characteristics. The segmentation process partitions an image into homogeneous regions, also called classes or subsets, considering one or more similar characteristics (Fu and Mui, 1981; Duda et al., 2000). Most of segmentation methods for medical images, are based on delineation of a curve that defines the anatomical structures, which allows to discriminate the structure of interest from other structures that appear in the image (Kervrann and Heitz, 1999). Another kind of techniques are based on application of classification methods, where the image is processed until represented as a non–overlapped set of two (2) regions (subject of interest and background) (Mitchell et al., 2001).

Images studies in cardiology are used to obtain both qualitative and quantitative information of the heart and vessels morphology and function. Several clinical parameters can be extracted from dynamics images of cardiovascular structures with the objective of reproducing the heart space–time behavior (Rabit, 2000). Assessment of cardiovascular function is important since Cardio–Vascular Disease (CVD) is considered the most important cause of mortality. Approximately 17 million people die each year, representing one third of the deaths in the world (WHO, 2002a). About 85% of overall mortality of middle- and low-income countries is due to CVD and it is estimated that CVD will be the leading cause of death

Bravo A., Clemente J., Vera M., Avila J. and Medina R. (2010).
A HYBRID BOUNDARY–REGION LEFT VENTRICLE SEGMENTATION IN COMPUTED TOMOGRAPHY.
In *Proceedings of the International Conference on Computer Vision Theory and Applications*, pages 107-114
DOI: 10.5220/0002849301070114

in developed countries in two years (WHO, 2002b).

Multi Slice Computerized Tomography is probably the term most commonly used to describe the latest developments in Spiral computed tomography (CT) which is based on simultaneous acquisition of more than one tomography plane, and it is closely related to acquisition systems with multiple detectors (Fuchs et al., 2000).

Left ventricle (LV) is considered the main cavity of the heart. In this sense, the assessment of the LV function allows to assess the cardiovascular function. The LV function analysis requires the accurate description of ventricular shape.

1.1 Related Work

There are several research studies on cardiac segmentation especially focused on left ventricle segmentation. Lynch *et al.* (Lynch et al., 2008) developed a LV segmentation method from magnetic resonance imaging. The method uses prior knowledge about ventricular motion to guide a parametric model of the cardiac cavity. The model deformation was initially controlled by a level–set formulation. The state of the model attained by the level–set evolution was refined using the expectation maximization (EM) algorithm. The objective was to fit the model to MRI data. The method was tested using a set of six clinical databases. The correlation coefficient obtained by a linear regression analysis of segmentation results with respect to manual segmentation was 0.76.

Fleureau *et al.* (Fleureau et al., 2006), reported a semi–automatic and multi–structure three–dimensional (3–D) segmentation method. The method was applied to extract the heart cavities from MSCT sequences. The method associated basic agents to the objects of interest. Each agent learnt the image region characteristics through a Support Vector Machine formulation. The cardiac cavities were obtained by maximizing the region associated to each basic agent. The approach allowed to discriminate structures such as, left ventricle, left atrium, right ventricle and right atrium. However, the clinical validation was not performed at the time of publication.

Chen *et al.*(Chen et al., 2004) developed a hybrid model for LV CT segmentation. The model couples a segmenter, based on a Gibbs prior models and deformable models with a marching cubes procedure. A external force based on a scalar gradient was considered in order to achieve convergence. The approach was tested using 8 CT studies. Results obtained reveals the good behavior of the method.

Recently, a semi–automatic segmentation method based on a 3–D active shape model has been proposed by Van Assen *et al.* (Assen et al., 2008). The method has the advantage of being independent with respect to the imaging modality. The LV shape was obtained for the whole cardiac cycle in 3D MRI and CT sequences. A point–to–point distance was one of the metrics used to evaluate the method performance. The average value of the distances obtained for the CT sequences was 1.85 mm.

1.2 Purpose

In this research, an automatic image segmentation approach useful to extract the left ventricle cavity from multi–slice computerized tomography 4–D (3–D + time) images is proposed. Morphological filters are used to improve the LV information in the images, and thus to facilitate the process of segmentation. The approach uses a region growing algorithm for the segmentation. A pixel called initial seed is located in the cavity of interest using the generalized Hough transform. This seed is established in the first volume of the MSCT dataset, and then compared with certain neighborhood pixels characteristics such as intensity and topological relationship according to a region–growing algorithm. The segmentation algorithm allows to obtain a binary image with the LV information and the background. From this initial binary image a new seed is automatically generated for segmenting the next MSCT volume. The first seed is then propagated along the 3–D image sequence to obtain the LV surfaces for all instants of the cardiac cycle.

2 METHOD

2.1 Dataset

A human MSCT database is used. The dataset contains 20 volumes to describe the heart anatomical information for a cardiac cycle. Each volume has 262 CT slices where the spacing between pixels is 0.488281 mm and the slice thickness is 0.625 mm. The data acquisition was triggered by the R wave of the ECG signal. Each image is quantized with 12 bits per pixel and the size is 512×512 pixels.

2.2 Hough Transform Seed Localization

In this work, the Generalized Hough Transform (GHT) is applied to obtain the left ventricle border in one MSCT slice. From this contour, the seed point required to initialize an unsupervised clustering algorithm is computed.

The GHT proposed by Ballard (Ballard, 1981) has been used to detect objects, with specific shapes, from images. The proposed algorithm consists of two stages: 1) training and 2) detection. During the training stage, the objective is to describe a pattern of the shape to detect. This pattern is parameterized using the gradient direction (θ) at each pattern point, the distance (r) between the reference point (x_c, y_c) and each pattern point, and the angle (α) with respect to x–axis of the line formed by the reference point and each pattern point. The parameters describing the shape are stored in an array known as the R–Table.

The second stage is implemented to detect a similar shape in an image not used during the training step. The parameter θ is calculated for each point in a pre–processed image to segment. The θ value is used as an entry to the R–table. The corresponding r and α values found in the table are used to compute the candidates to reference points (x_c, y_c) according to 1.

$$\begin{aligned} x_c &= x + r\cos(\alpha) \\ y_c &= y + r\sin(\alpha) \end{aligned} \quad , \tag{1}$$

where (x, y) are object boundaries points. An accumulator is used to count the occurrences of each reference point calculated. The reference point with more occurrence is selected.

The overviews of the training and detection stages for the LV segmentation are shown on the flowcharts in Figures 1 and 2. In the training stage, the heart structures boundaries are initially estimated using the Canny edge detection algorithm (Canny, 1986). The LV contour is manually labeled in the Canny's contours map. The centroid of the LV contour is used as the reference point (x_c, y_c). The R–table is constructed when the values of the (θ, r, α) are computed.

During the detection step (Figure 2), the application of the Canny edge detection algorithm is also required. A thresholding technique is applied in order to discriminate the size of the regions delimitated by the borders labeled in the Canny image. The thresholds used correspond to areas measured in pixels. The regions obtained after the thresholding are considered as candidates for the left ventricle shape. The border points of the LV candidates are used to calculate the gradient direction (θ). For the θ values found in the R–table, the corresponding r and α values are used to calculate the reference points using 1. The final contour correspond to the candidate whose reference point has the best match with respect to the reference point of the pattern.

Figure 3 illustrates the training process applied to one MSCT slice while Figure 4 shows the results of the segmentation for other MSCT slice.

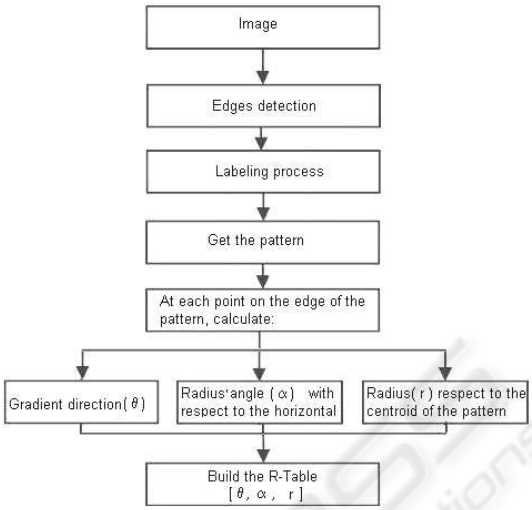

Figure 1: GHT training stage.

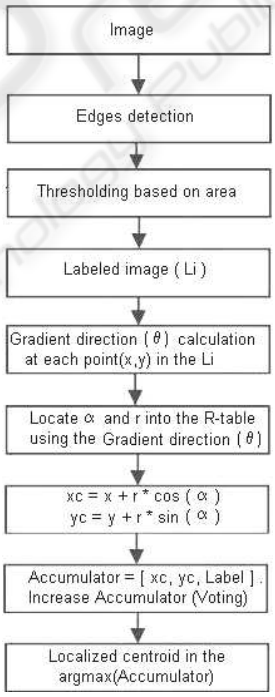

Figure 2: GHT detection stage.

2.3 Unsupervised Segmentation

2.3.1 Pre-processing

Mathematical morphological operators are used for implementing the filters aimed at enhancing the LV information. These morphological operators are based on non–linear operations between the original image (**I**) and a set of additional points known as structuring element (**B**) (Serra, 1982). The applied filters are based on the top–hat transform. This trans-

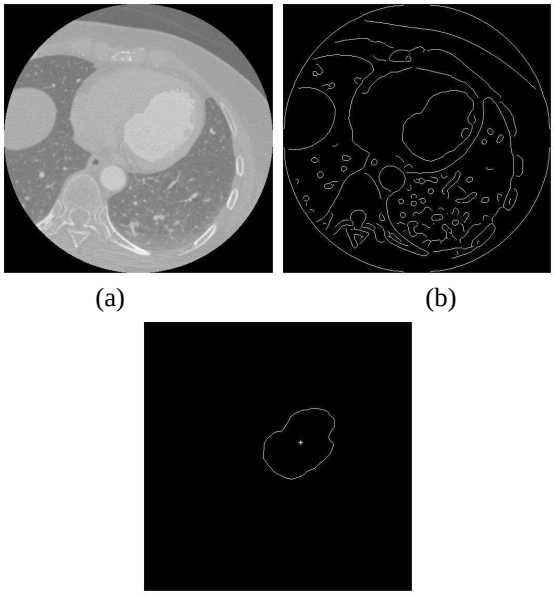

(a) (b)

(c)

Figure 3: Results of GHT training stage. (a) Original image. (b) Canny image. (c) Pattern obtained.

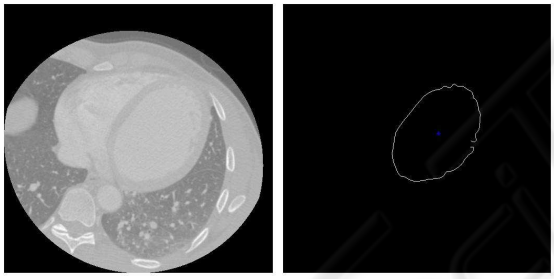

(a) (b)

Figure 4: Results of GHT segmentation stage. (a) Original image. (b) LV segmented.

form is a composite operation defined by the set difference between the image processed by a closing operator and the original image. The closing ($\bullet$) operator is also a composite operation that combines the basic operations of erosion ($\ominus$) and dilation ($\oplus$). The top–hat transform is expressed according to (2).

$$\mathbf{I} \bullet \mathbf{B} - \mathbf{I} = (\mathbf{I} \oplus \mathbf{B}) \ominus \mathbf{B} - \mathbf{I} \ . \qquad (2)$$

A modification of the basic top–hat transform definition is introduced. A Gaussian filter is applied to the original image. The discrete Gaussian operator with standard deviation σ is used as a filter mask (3).

$$K(i,j) = \left(\frac{1}{2\pi\sigma^2}\right) e^{-\frac{i^2+j^2}{2\sigma^2}}; 0 \leq i,j \leq n \ , \qquad (3)$$

where n denotes the mask size and σ is set as the standard deviation of the original image. The processed

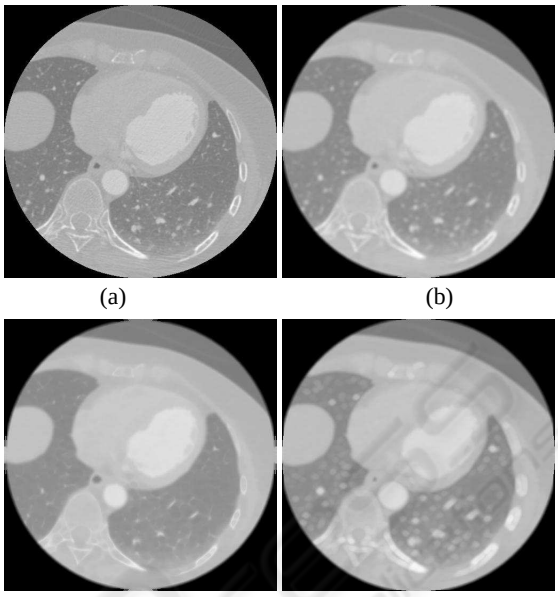

(a) (b)

(c) (d)

Figure 5: Pre–processing stage. (a) Original image. (b) Gaussian smoothed image. (c) Eroded image. (d) Dilated image.

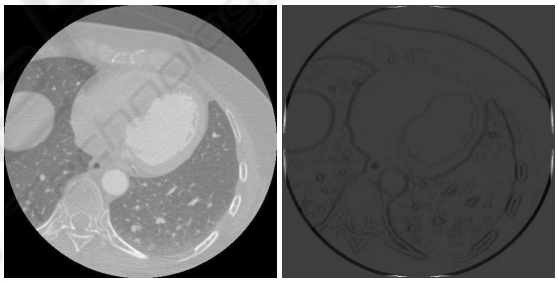

(a) (b)

Figure 6: The top–hat transform. (a) Original image. (b) Processed image.

image ($\mathbf{I}_{\text{Gauss}}$) is a blurred version of the input.

The Gaussian smoothed image is used to calculate the morphological closing. The structuring element selected is an ellipsoid that varies in size depending on the operator. The major axis of the structuring element used for the erosion is 3 and for the dilation is 5. Figure 5 shows part of the pre–processing stage.

Finally, the top–hat transform is calculated using (4), the result is an image with enhanced contours. The original image and the processed image are shown in Figure 6.

$$\mathbf{I}_{\text{BTH}} = (\mathbf{I}_{\text{Gauss}} \oplus \mathbf{B}_5) \ominus \mathbf{B}_3 - \mathbf{I}_{\text{Gauss}} \ . \qquad (4)$$

The intensity values of the top–hat image ($\mathbf{I}_{\text{BTH}}$) and the Gaussian image ($\mathbf{I}_{\text{Gauss}}$) are used to create a feature vector. This feature vector is used to construct

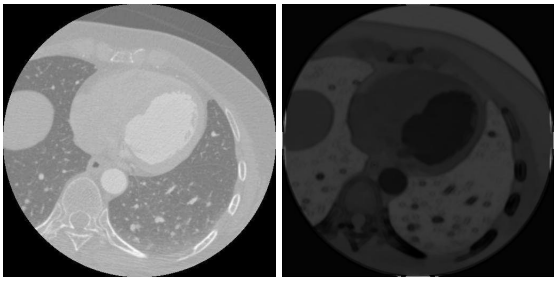

(a) (b)

Figure 7: Final enhancement process. (a) Original image. (b) Similarity image.

a similarity matrix based on a similarity criteria (Haralick and Shapiro, 1992). The criteria measures the difference between the gray–level values of pixels in $\mathbf{I}_{\text{BTH}}$ and the smoothed image, $\mathbf{I}_{\text{Gauss}}$. According to this criteria, pixels $p_1(x,y)$ (in $\mathbf{I}_{\text{BTH}}$) and $p_2(x,y)$ (in $\mathbf{I}_{\text{Gauss}}$) have features vectors denoted as: $\mathbf{pv}_1 = [i_1, a]$ and $\mathbf{pv}_2 = [i_2, b]$, where i_1 and i_2 denote the intensity associated with the corresponding pixel of $\mathbf{I}_{\text{BTH}}$ and, a and b are the intensity of the smoothed image. The pixel values in the similarity matrix are obtained by using the following expression:

$$p_{\mathbf{I_S}}(x,y) = (i_1 - i_2)^2 + (i_1 - b)^2 + (i_2 - a)^2 \quad . \quad (5)$$

Figure 7 shows the image enhanced using the similarity criteria, where the information related to the LV cavity is enhanced with respect to other anatomical structures that are present in the MSCT slice.

The process described previously, is applied to all volumes of the human MSCT database. Since this process requires large computing resources, multiprogramming based on threads is used to speed up the enhancement. The performance and a speed test is applied using 1Gb memory–Pentium IV machine. An optimal reduction of 48% in processing time, without saturating the equipment operation, is attained using 4 threads.

2.3.2 Segmentation Stage

A region growing technique is used to segment the LV. The unsupervised clustering algorithm requires a seed point located inside the region of interest to identify the cardiac cavity. The seed is established in one slice at only one time instant of the MSCT 4–D image sequence. The procedure used to establish the seed point is based on the GHT (see section 2.2).

Seed Determination. A seed is used for starting the region–growing segmentation process. This seed corresponds to the reference point of the shape obtained using the GHT procedure. The seed point is located in the bi–dimensional (2–D) image $\mathbf{I}_k^t$, where t represents the time instant of the MSCT dataset, and k is the slice in the corresponding volume t. When the image $\mathbf{I}_k^t$ has been segmented (process described in section 2.3.2) a binary image ${}^{\text{b}}\mathbf{I}_k^t$ is obtained. In this image, pixels in white represent the segmented region. From ${}^{\text{b}}\mathbf{I}_k^t$ the seed points necessary to segment the entire volume t are estimated. The center of mass of the segmented region in the image ${}^{\text{b}}\mathbf{I}_k^t$ is calculated and denoted as $r(x,y)$. The pixel $r(x,y)$ is the new seed to segment the images $\mathbf{I}_{k+1}^t$ and $\mathbf{I}_{k-1}^t$. The seed generation process is applied upward by diminishing the value of k until reaching the LV base. In the same way, the process is applied downward by increasing k until reaching the apex.

The process for propagating the seed from one volume to the next, is also based on the calculation of the gravity center as previously explained. However, in this case the calculation is performed for the 3-D binary object.

The procedure based on calculation of the center of mass, results in a point located very near of the LV anatomical axis. In consequence, the seed is always located inside the target region (inside the LV).

Region Growing Algorithm. The algorithm is developed using dynamic linked–lists. The algorithm inputs are the enhanced image and a binary image with all pixels set to zero (0). The lists are implemented as a First In First Out (FIFO) queue. The list is used to store temporarily the pixels that fulfill the clustering criterion. The objective is to develop an iterative algorithm highly efficient with respect to memory requirements aiming at avoiding memory overflows. Each node in the list contains the pixel information: location and gray level intensity. The first node inserted in the list is the seed pixel.

After introducing the seed pixel in the FIFO list, the algorithm performs the following steps: 1) the first node of the list is dequeue, 2) the gray level information associated to the analyzed node is compared with pixel intensities in an 8 pixels neighborhood to determine if these neighbor pixels belong or not to the target region. Pixels of the neighborhood that fulfill the clustering criterion are inserted at the end of the list and their values in the binary image are modified to one (1). The pixels that do not fulfill with the condition are rejected, and 3) the algorithm continues with this process while there are nodes in the list. The algorithm output is the binary image where pixels set to one represent the segmented region. The uniformity criterion for grouping pixels is as follows: pixels are grouped if the difference between the pixel value in the neighborhood and the intensity of the pixel extracted of the list is below $\frac{1}{4}$ standard deviation of sim-

ilarity image.

In this algorithm multiprogramming is also used, considering two threads. The first thread segments the slices from $\mathbf{I}_k^t$, $\mathbf{I}_{k+1}^t$,....., to $\mathbf{I}_{apex}^t$, and the second thread segments the slices from the $\mathbf{I}_{k-1}^t$, $\mathbf{I}_{k-2}^t$,....., to $\mathbf{I}_{base}^t$. The LV base and apex are detected automatically by our algorithm. A comparison between current segmented area and previous segmented area is performed. If the areas are different in more than 80%, the current segmented area does not belong to the interest region, and then the segmentation process is stopped. Figure 8 shows the results of the segmentation for two consecutive tomographic slices.

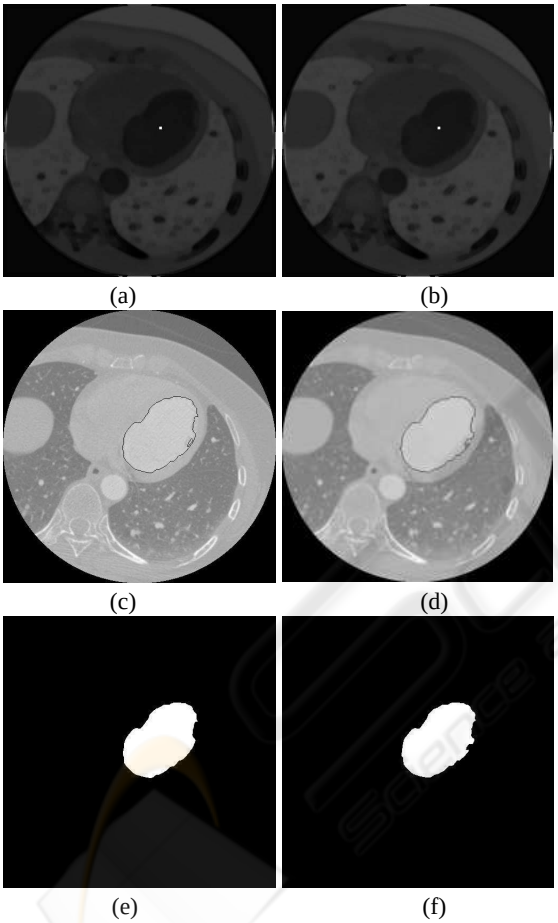

Figure 8: (a) Seed in slice $\mathbf{I}_k^t$. (b) Seed in slice $\mathbf{I}_{k+1}^t$. (c) and (d) LV contours. (e) and (f) LV areas.

After the segmentation process the reconstruction of the LV surface is performed using the Visualization Toolkit (VTK) (Schroeder et al., 2001). The endocardial LV wall is reconstructed using the marching cubes algorithm (Salomon, 1999) (Figure 9).

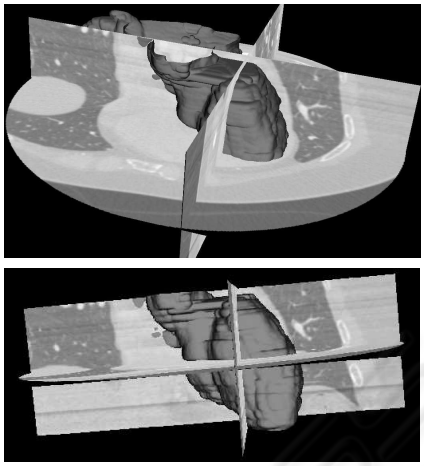

Figure 9: Result of the segmentation process.

2.3.3 Validation

The proposed method is validated by calculating the difference between the estimated LV shape with respect to a ground truth shape, traced by an expert. Two different methodologies for evaluating the performance of the LV segmentation method are considered. First, the approach proposed by Suzuki *et al.* (Suzuki et al., 2004) is incorporated. Suzuki's quantitative evaluation methodology is based on calculating two metrics that represent the contour error (E_C) and the area error (E_A). See (Suzuki et al., 2004, p. 335) to show the contour and area errors expressions.

The validation methodology proposed by Chalana and Kim (Chalana and Kim, 1997) is also used. A metric based on a mean absolute distance (MAD) of the distance to the closest point (DCP) is used for assessing the position error (E_P) between contours automatically extracted with respect to contour traced by an experts. The metric expression can be found in (Chalana and Kim, 1997, p. 643).

3 RESULTS

The proposed method is implanted using a multi–platform object–oriented methodology along with C++ multiprogramming and using dynamic memory handling. Standard libraries such as the Visualization Toolkit (VTK) are used. VTK consists of a complete set of algorithms for 3–D images visualization. The Fast Light Toolkit (FLTK) open source libraries are also used to develop the graphic interface. The code is executed in Microsoft Windows and Linux platforms. In the application, threads are used to speed up the process and then to optimize the response times.

The segmentation algorithms are tested with more

Figure 10: Cardiac structures at 10%, 30%, 50%, 70% and 90% of the cardiac cycle.

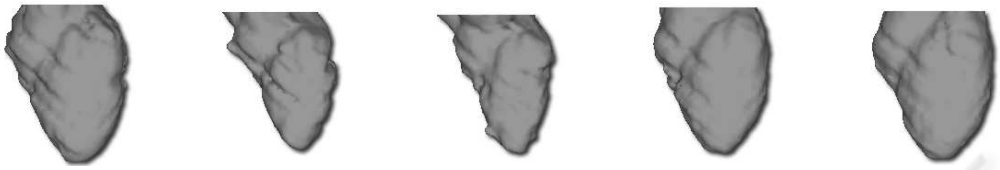

Figure 11: Left ventricle surfaces in the new frame of reference.

Table 1: Errors obtained for a total of 262 images processed.

Error Types	Result
E_A	3.38 % $\pm$ 3.09 %
E_C	6.23 % $\pm$ 3.77 %
E_P	1.52 mm $\pm$ 0.18 mm

than ten thousand 2–D images, obtaining good results for all images with very satisfactory processing times. For instance, for a database including 20 volumes and 262 images per volume, the filtering and segmentation take approximately 15 minutes. Figure 9 shows the segmented LV overlaid with three orthogonal slices extracted from the original database (axial, coronal and saggital), where it can be shown that for these planes the structure matches with the LV contours.

Table 1 shows the comparison of extracted surface with respect to the surface traced by the cardiologist. The errors estimated are expressed as $mean \pm standard\ deviation$. The position error varies between 0.87 mm and 1.72 mm. The average position error obtained using our segmentation method was 1.52 mm which is smaller than the average error (1.85 mm) reported by Van Assen *et al.* (Assen et al., 2008). Using the proposed segmentation method the average contour error and the average area error are 6.23% and 3.38%, respectively.

Additionally, the application allows to establish a particular frame of reference not dependent on the original position of the heart. This frame is based on an axis (z–axis) joining the apex to the joint between the mitral and aortic valves as determined in the endocardial LV wall, and a plane perpendicular to this axis that is the x–y plane. The frame of reference corresponds with the image acquisition geometry for the MRI images. Figure 10 shows the segmentation results while Figure 11 shows the left ventricle in the new frame of reference. The LV structures for instants located at 10%, 30%, 50%, 70% and 90% of the cardiac cycle are shown.

4 CONCLUSIONS

An automatic method for LV image segmentation from 4–D MSCT datasets was proposed. The software system is a platform independent tool developed using C++ and open–source libraries. The pre–processing stage was based on gray level mathematical morphology filters aimed at performing the smoothing and enhancement of image contours. A region growing algorithm was controlled by a seed point located in one volume using generalized Hough transform, which was propagated to the rest of volumes in order to segment the entire MSCT database.

A valuable contribution was the utilization of threads since they improve the processing time for the whole process. The segmentation method evaluation was performed by comparing the estimated contours with respect to contours traced by a cardiologists. The comparison was performed based on the methodologies proposed in (Chalana and Kim, 1997; Suzuki et al., 2004) which are also used in (Oost et al., 2006) and (Bravo and Medina, 2008). The validation stage shows that errors are small. The method allowed to detect LV important features as the papillary muscles.

As a future research we propose to use the method for automatic segmentation of right ventricle, left and right atrium in multi–slice computerized tomography (MSCT) images. Additionally, we plan to develop the approach in a 3–D domain in order to take into account three–dimensional topological features of the left ventricle and for speeding up the segmentation procedure. We also have considered to use the proposed method for heart structures segmentation in other cardiac imaging modalities.

ACKNOWLEDGEMENTS

The authors would like to thank the Investigation Dean's Office of Universidad Nacional Experimental del Táchira, LOCTI grant PR0100401, and CDCHT from Universidad de Los Andes (projects I-1075-07-02B and NUTA C–24–07–02–C) for their support to this research. Authors would also like to thank H. Le Breton and D. Boulmier from the Centre CardioPneumologique and M. Garreau from Laboratoire Traitement signal et de l'image (LTSI) in Rennes, France for providing the human MSCT database.

REFERENCES

Angelini, E., Laine, A., Takuma, S., Holmes, J., and Homma, S. (2001). LV volume quantification via spatiotemporal analysis of real–time 3–D echocardiography. *IEEE Trans. Med. Imag.*, 20(2):457–469.

Assen, H. V., Danilouchkine, M., Dirksen, M., Reiber, J., and Lelieveldt, B. (2008). A 3D active shape model driven by fuzzy inference: Application to cardiac CT and MR. *IEEE Trans. Inform. Technol. Biomed.*, 12(5):595–605.

Ballard, D. (1981). Generalizing the hough transform to detect arbitrary shapes. *Pattern Recog.*, 13(2):111–122.

Bankman, I. (2000). *Handbook of Medical Imaging: Processing and Analisys*. Academic Press, San Diego.

Bravo, A. and Medina, R. (2008). An unsupervised clustering framework for automatic segmentation of left ventricle cavity in human heart angiograms. *Comput Med Imaging Graph.*, 32(5):396–408.

Canny, J. (1986). A computational approach to edge detection. *IEEE Trans. Pattern Anal. Machine Intell.*, PAMI–8:679–698.

Chalana, V. and Kim, Y. (1997). A methodology for evaluation of boundary detection algorithms on medical images. *IEEE Trans. Med. Imag.*, 16(5):642–652.

Chen, T., Metaxas, D., and Axel, L. (2004). 3–D cardiac anatomy reconstruction using high resolution CT data. In *Proc. MICCAI (1)*, pages 411–418.

DICOM (1999). Digital imaging and communication in medicine DICOM. NEMA Standards Publication.

Duda, R., Hart, P., and Stork, D. (2000). *Pattern Classification*. Wiley–Interscience, New York.

Field, M. J. (1996). *Telemedicine: A Guide to Assessing Telecommunications in Health Care*. Institute of Medicine, National Academy Press, Washington.

Fleureau, J., Garreau, M., Hernández, A., Simon, A., and Boulmier, D. (2006). Multi-object and N-D segmentation of cardiac MSCT data using SVM classifiers and a connectivity algorithm. In *Computers in Cardiology*, pages 817–820.

Fu, K. S. and Mui, J. K. (1981). A survey on image segmentation. *Pattern Recog.*, 13(1):3–16.

Fuchs, T., Kachelriess, M., and Kalender, W. (2000). Systems performance multislice spiral computed tomography. *IEEE Eng. Med. Biol. Mag.*, 19(5):63–70.

Haralick, R. A. and Shapiro, L. (1992). *Computer and Robot Vision*, volume I. Addison–Wesley, USA.

Kervrann, C. and Heitz, F. (1999). Statistical deformable model–based segmentation of image motion. *IEEE Trans. Image Processing*, 8(4):583–588.

Lynch, M., Ghita, O., and Whelan, P. (2008). Segmentation of the left ventricle of the heart in 3-D+t MRI data using an optimized nonrigid temporal model. *IEEE Trans. Med. Imag.*, 27(2):195–203.

Mitchell, S., Lelieveldt, B., van der Geest, R., Bosch, H., Reiber, J., and Sonka, M. (2001). Multistage hybrid active appearance model matching: Segmentation of left and right ventricles in cardiac MR images. *IEEE Trans. Med. Imag.*, 20(5):415–423.

Nelson, T. R. and Elvins, T. T. (1993). Visualization of 3D ultrasound data. *IEEE Comput. Graph. Appl.*, 13(6):50–57.

Oost, E., Koning, G., Sonka, M., Oemrawsingh, P. V., Reiber, J. H. C., and Lelieveldt, B. P. F. (2006). Automated contour detection in X–ray left ventricular angiograms using multiview active appearance models and dynamic programming. *IEEE Trans. Med. Imag.*, 25(9):1158–1171.

Rabit, O. (2000). Quantitative analysis of cardiac function. In Bankman, I. N., editor, *Handbook of Medical Imaging: Processing and Analysis*, pages 359–374. Academic Press, San Diego.

Salomon, D. (1999). *Computer Graphics and Geometric Modeling*. Springer Verlag, New York.

Schroeder, W., Martin, K., and Lorensen, B. (2001). *The Visualization Toolkit, An Object-Oriented Approach to 3D Graphics*. Prentice Hall, New York.

Serra, J. (1982). *Image Analysis and Mathematical Morphology*. A Press, London.

Suzuki, K., Horiba, I., Sugie, N., and Nanki, M. (2004). Extraction of left ventricular contours from left ventriculograms by means of a neural edge detector. *IEEE Trans. Med. Imag.*, 23(3):330–339.

WHO (2002a). Integrated management of cardiovascular risk. The World Health Report 2002 Geneva, World Health Organization.

WHO (2002b). Reducing risk and promoting healthy life. The World Health Report 2002 Geneva, World Health Organization.